JMEPEG (2006) 15:742-749
DOI: 10.1361/105994906X150867

1059-9495/$19.00

Effect of Corrosion on Mass Loss, and High and Low Cycle Fatigue of Reinforcing Steel

Ch. Alk. Apostolopoulos and D. Michalopoulos

(Submitted March 7, 2006)

The effect of various levels of corrosion on the mass loss, and the high and low cycle fatigue of $BSt500_s$ steel reinforcement were experimentally investigated. The mass loss, the fatigue limit, and the life expectancy were reduced by 1.5 to 2.9%, 20 to 40%, and 56 to 76%, respectively, according to the corrosion level. Low cycle strain-controlled fatigue testing under a ±1% constant amplitude strain showed that the corroded steel bars exhibit a gradual reduction in the load-bearing ability, the available energy, and the number of cycles to failure. The considerable reduction in the fatigue limit took place because the mass loss led to a reduction of the exterior hard layer of martensite and a drastic drop in the energy density of the corroded specimens, thus developing stress concentration points that are highly localized at imperfections, and especially in the pits and notches of the rib bases of the corroded steel. Because corrosion and cycle fatigue are time-dependent, it seems that steel reliability is also time-dependent.

Keywords $BSt500_s$ steel, fatigue, low cycle fatigue, mass loss, salt spray corrosion

1. Introduction

The reinforcing steel of concrete structures becomes vulnerable to damage and high repair costs when exposed to corrosion. Corrosion is an electrochemical process during which metallic iron is converted to rust, creating volumetric expansion of the steel bars and also causing extremely high tensile forces within the concrete cover. This results in crack formation from the steel bar to the concrete surface or between bars, allowing oxygen and moisture to attack the bars faster and to increase the corrosion rate. The rust reduces the bond strength and results in the loss of steel-concrete composite action, which affects the serviceability and performance of structures (Ref 1-5).

The gradual degradation of the integrity of concrete structures is related to the accumulated detrimental effect of corrosion resulting in serious financial losses because corrosion causes concrete cracking and the eventual deterioration of the structure before the end of its design life. While steel corrosion is the main issue affecting concrete durability, the relationship between corrosion level and load-carrying capacity of structural members has not been established yet. Steel corrosion and the associated cracking and spalling of concrete have been identified as the most severe forms of deterioration. At rebar corrosion values of approximately 7 and 12%, the rib profile losses are approximately 45 and 70%, respectively, which explains the steel bar slippage mode of failure. Corrosion levels of 5 and 7% are observed to cause significant increases in crack width and rib profile loss and a 30 to 70% reduction in bond strength. A crack width of about 0.30 mm and a 25% rib profile loss appear to be the threshold beyond which a sharp reduction in bond strength occurs (Ref 6, 7).

Seismic loads act on the load-bearing elements of structures in the form of high strain reversals, which can be simulated as single-axis, low cycle fatigue (Ref 8). The Fourier spectra (Ref 8, 9) of ground movement during an earthquake that occurred in Japan showed that the loading was cyclic and the frequency corresponding to the maximum amplitude was approximately 2 Hz. Investigation of the catastrophic earthquake of Tang Shan in China confirmed that the failure mode of the structural steel of the building was low cycle fatigue (Ref 8). During seismic movement, structures are subjected to alternating shear forces and bending moments. This cyclic motion results in the gradual bursting and detachment of the concrete cover, which finally leaves the reinforcing steel bars as the sole load-bearing elements, thus forcing them to carry both the shear forces and the bending moments leading to permanent plastic deformation of the steel. These deformations increase due to continuous dynamic loading while the compressive concrete zone is annihilated (Ref 10).

In coastal locations, the climatic conditions constitute one of the most aggressive environments for concrete structures due to the severe ambient salinity, high temperature and humidity, and also the ingress of chlorine through wind-borne salt spray (Ref 7, 11). Chloride-induced damage of reinforcing steel results in concrete cracking and spalling, the destruction of the protective steel barrier, and the formation of pits, notches, and cavities on the steel surface. Durability is one of the most important merits of using reinforced concrete; however, the formation of cracks causes corrosion of the steel bars and initiation of a serious problem, which becomes more severe in harsh environments. Even though the impact of corrosion on the strength of steel reinforcing bars is well known, the current design codes do not address the problem because they are unable to quantify it and need further review. Quantification of the corrosion and mass loss of steel with the reduction of its mechanical properties has been attempted (Ref 11, 12). The annual repair cost for highway bridges in the United States due to soluble chlorides, including steel and concrete, is estimated

Ch. Alk. Apostolopoulos and **D. Michalopoulos,** Department of Mechanical Engineering and Aeronautics, University of Patras, Patras, Greece 26500. Contact e-mail: mixalop@mech.upatras.gr.

Table 1 Mechanical properties of steel $BSt500_s$ specimen

Material yield stress, MPa	Tensile strength, MPa	Elastic modulus, GPa	Elongation (after breaking), %
Ribbed bar ≥500	≥550	200	≥12

to be $8.3 billion, while the corresponding cost for highways is $20 billion (Ref 13, 14). Life-cycle analysis estimates the indirect costs to the user due to traffic delays and lost productivity at more than 10 times the direct cost.

Reinforced concrete structures are seriously affected by steel corrosion due to exposure to chlorides from seawater, salt and saltwater, deicing chemicals, brackish water, or spray from these sources. In addition, steel-concrete bonding is greatly reduced through deterioration of the steel, the concrete, or both (Ref 5, 15). Rust resides at the interface between steel reinforcement and concrete, degrading their bond and also reducing the useful life of the structure. The reduction in the structural performance of reinforced concrete members due to corroded steel is caused by the loss in the effective cross-sectional area of concrete due to cracking in the cover concrete, loss of the mechanical properties (Ref 11, 12), and the performance of reinforcing bars due to the reduction of their cross-sectional area and also the loss of bonding (Ref 5, 15, 16).

The low cycle fatigue of rebar occupies a large amount of the research that has been undertaken. It is felt that these results still need time and work to be properly processed to arrive at a quantitative analytical model that is able to embrace all of the features that have only been qualitatively described (Ref 17-20). The level of corrosion of steel bars affects their durability and performance, and shortens the design life of structures (Ref 21-24). In the current study, the impact of corrosion on mass loss, and high and low cycle fatigue properties of $BSt500_s$ steel bars was evaluated.

2. Experimental Procedure

2.1 Experimental Corrosion

$BSt500_s$ tempcore steel in maximum permissible values of the final product contains Carbon (C) = 0.240%, Phosphorus (P) = 0.055%, Sulfur (S) = 0.055%, and Nitrogen (N) = 0.013% with the mechanical properties shown in Table 1. Tempcore is a patented mill process that produces high-strength reinforcing rebar via in-line quenching and self-tempering.

Ribbed steel bars 12 mm in diameter were artificially corroded in a specially designed salt spray corrosion chamber, according to the ASTM B117-94 standard (Ref 25) for 10, 20, 30, 45, 60, and 90 days. To accelerate corrosion, the specimens were sprayed in a 5% sodium chloride and a 95% distilled water solution, with pH range of 6.5 to 7.2 and a spray chamber temperature of $35 \pm {}^{1.1}_{1.7}$ °C for different exposure times so that different corrosion levels were obtained. Pitting was observed to have started progressively on the specimens after 10, 20, and 30 days, a corrosion level that became progressively more severe. After salt spray exposure, the specimens were washed with clean water according to the ASTM G 1-72 procedure to remove any leftover salt deposits from their surface and then dried. Figure 1 shows the cross section of a 12 mm diameter steel bar, where the hard martensite constituent is followed by the softer bainite and ferrite/pearlite microstructure layers.

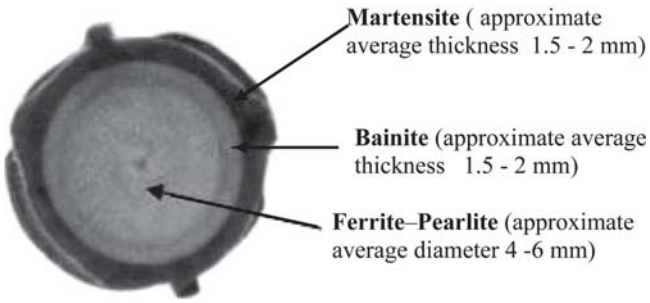

Fig. 1 Cross section of reinforcing steel bar type $BSt500_s$, 12 mm in diameter

2.2 Mass Loss

The degree or level of corrosion was measured as the mass loss of the steel bars before and after completion of the corrosion tests. The bars were weighed and the percentage mass loss was calculated as follows:

$$M_l = \frac{M_i - M_f}{M_i} \times 100 \quad \text{(Eq 1)}$$

where M_l is the percent mass loss and M_i and M_f are the masses (in grams) of the noncorroded and corroded specimens, respectively. The relationship between the remaining mass and the corrosion duration for corroded versus noncorroded specimens is shown in Fig. 2, including the corresponding average cross-sectional area A_s of the specimens along with the mass loss. The area A_s was used in the calculation of the fatigue stress and was determined according to Deutsches Institut für Normung (DIN) 488-3 specification by:

$$A_s = \frac{1.274 \times M_f}{l} \quad \text{(Eq 2)}$$

where A_s is the cross-sectional area in square millimeters, M_f is the mass in grams, and l is the length in millimeters. The corrosion process created pitting, and formed cavities and notches on the steel surface, especially the rib bases, which became more severe as the corrosion duration increased. A more detailed examination of the mass loss extended to 90 days, a corrosion level that was considered necessary to gain enough insight into this process.

The micrographs of Fig. 3 show that pitting developed on the steel surfaces even after removal of the corrosion products. The relatively large pits that developed after 60 days of salt spray exposure suggest that these are the active sites at which corrosion is primarily taking place. The pitting appeared to be initiated at the reinforcement veins of the steel bars and proceeded to the intermediate space.

The gradual decrease of the strength characteristics is related to the mass loss, in particular that of the more resistive martensitic outer layer. It is well known that the high strength of the steel examined in the present investigation is mainly due to the presence of martensite (Ref 11). The micrographs in Fig. 4 show the gradual decrease of the thickness of the martensitic outer shell with increasing corrosion duration.

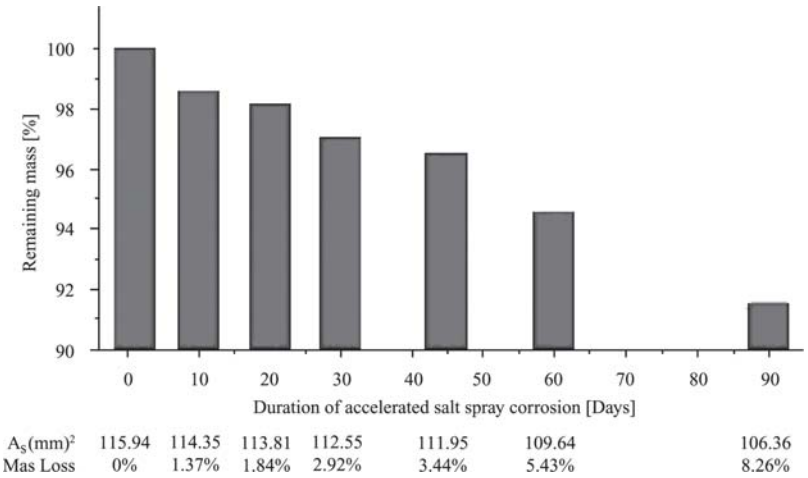

Fig. 2 Impact of corrosion on mass loss

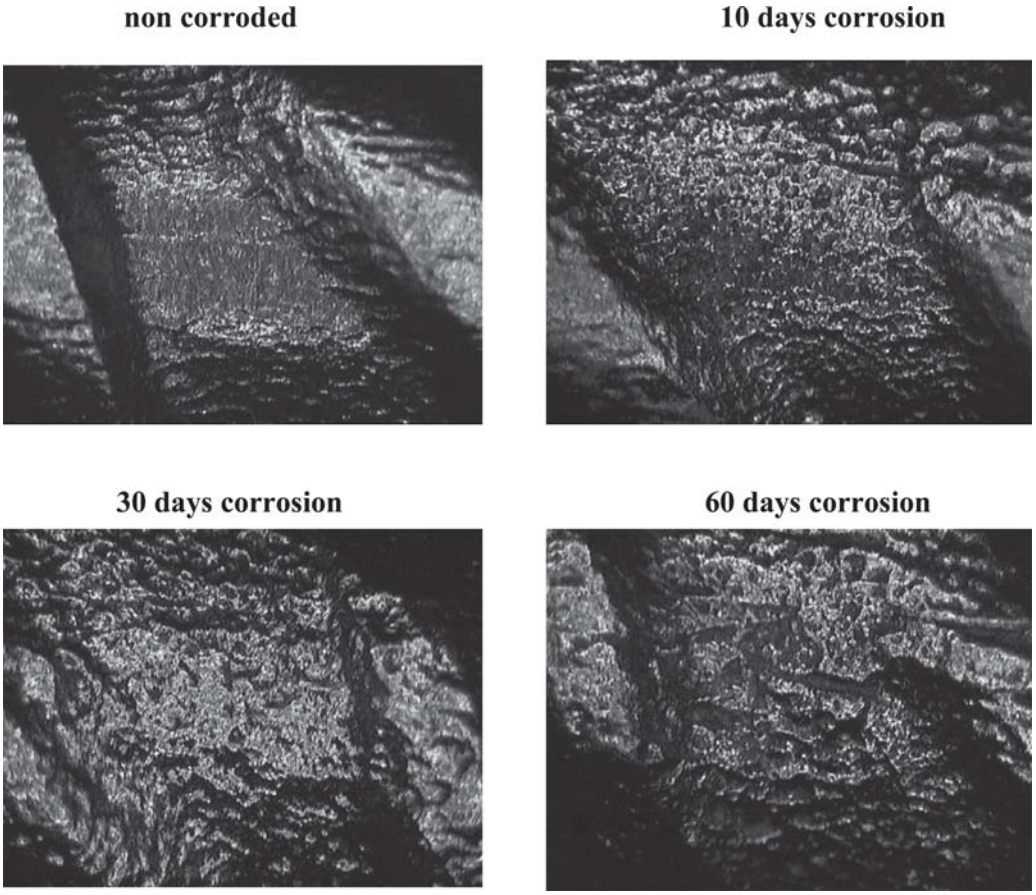

Fig. 3 Stereoscopic images of specimens

2.3 High Cycle Fatigue

The effect of corrosion on the fatigue and life expectancy of reinforcing steel bars was investigated through a series of 60 laboratory experiments. After the salt spray corrosion process, the uniaxial fatigue of the specimens was measured on servo hydraulic testing machine according to the ISO/FDIS 15630-1 method. These tests were carried out at fatigue levels of ±325, ±265, and ±200 MPa, a stress ratio $R = -1$, and a frequency of 20 Hz, and the conventional fatigue limit was determined for a life expectancy of $N_f = 8.1 \times 10^6$ cycles. These tests were performed in noncorroded and corroded specimens that had been exposed to salt spray for 15 and 30 days, respectively, and that resulted in three Woehler curves, utilizing 12 tests in each group of 20 tests for their construction, while the remaining eight tests were spares. The minimum length of the 12 mm diameter specimens had to be 14xd, but the ones used were 280 mm long, of which 55 mm was used under each grip and 170 mm was the free length used to facilitate loading into the testing machine. The experimental results are displayed in Fig. 5

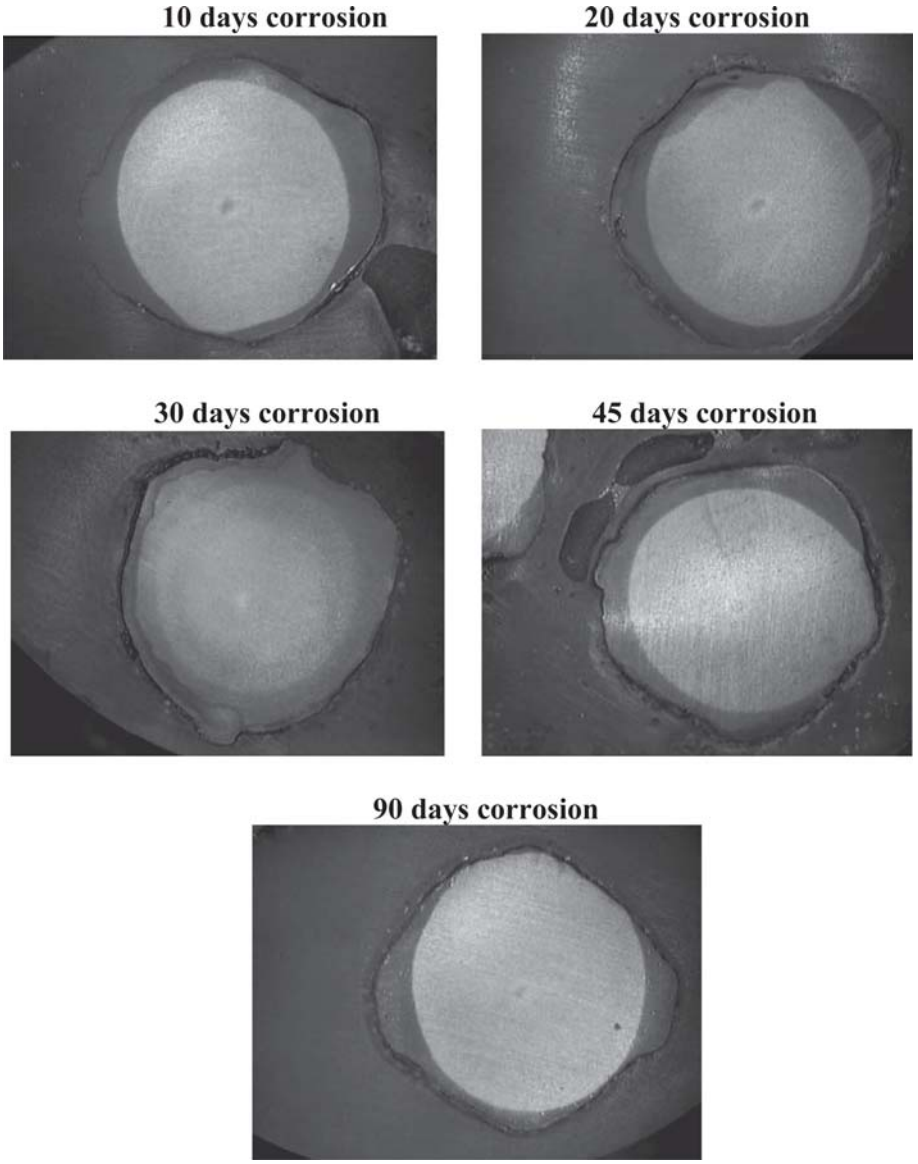

Fig. 4 Decrease of the martensitic layer as a result of corrosion duration

and 6 through Woehler S-N diagrams for samples that were noncorroded and corroded for 15 and 30 days on semilogarithmic and nonlogarithmic scales, respectively; the progressive reduction in fatigue strength can be realized as a function of the corrosion level. The curves of Fig. 6 are described satisfactorily with Weibull functions, the constants of which are shown in Table 2.

Figure 7 shows that the endurance limit for specimens corroded for 15 and 30 days versus noncorroded ones was reduced by 20 and 40%, respectively.

2.4 Low Cycle Fatigue

The effect of corrosion on the low-cycle fatigue behavior of $BSt500_s$ tempcore steel under earthquake conditions was investigated. Twenty-one specimens were subjected to uniaxial sinusoidal loads of 1 Hz frequency and a constant strain amplitude of ±1% after being exposed to a salt spray environment for different exposure times. The 12 mm diameter specimens for the low-cycle fatigue tests that were performed were cut into 172 mm lengths, and the free length between the grips was set at $6 \times 12 = 72$ mm. No buckling was observed. The section of the specimens has a transition zone between the core (ferrite-pearlite) and the external zone (ring of martensite).

Any modification in the geometry so as to comply with the standards for strain-controlled fatigue testing, such as that of the ASTM E606 standard (Ref 26), would alter the nature of the material, thus giving misleading results. Therefore, the specimens were subjected to low-cycle fatigue testing without modification of their cross-sectional area. The analytical expression for total strain is given by Basquin and Coffin-Manson (Ref 27):

$$\frac{\Delta\varepsilon_t}{2} = \frac{\Delta\varepsilon_e}{2} + \frac{\Delta\varepsilon_P}{2} = \frac{\sigma'_f}{E}(2N)^b + \varepsilon'_f(2N)^c \quad \text{(Eq 3)}$$

where $\Delta\varepsilon_t$, $\Delta\varepsilon_e$, and $\Delta\varepsilon_p$ are the total, elastic, and the plastic strain amplitudes, respectively, as shown in the steady-state loops of Fig. 8, and ε'_f and c are the fatigue ductility coefficient

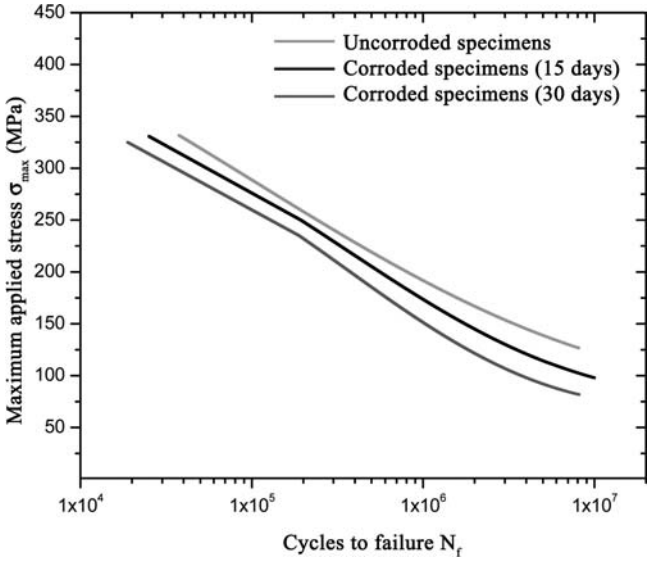

Fig. 5 Woehler S-N fatigue diagrams for noncorroded and corroded specimens

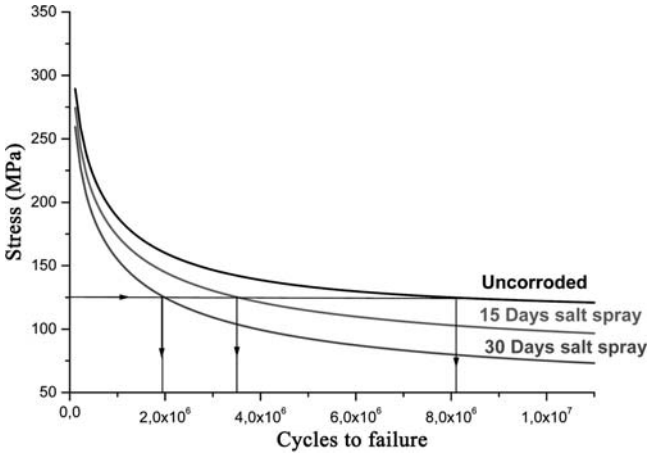

Fig. 6 Woehler S-N fatigue diagrams for noncorroded and corroded specimens

Table 2 Weibull constants

Constants	Noncorroded	15 days salt spray	30 days salt spray
C1	113.50884	75.97808	50.65955
C2	379.73621	401.14345	383.98002
C3	5.78098	5.78626	5.82995
C4	6.46082	5.16244	5.25499

and exponent, respectively, while σ_f' and b are the fatigue strength coefficient and exponent, respectively, and E is the modulus of elasticity. Three typical low-cycle fatigue stress-strain diagrams of 14 to 24, 340 to 350, and 535 to 545 cycles are shown in Fig. 8 where the progressive reduction of stress is observed. From the low-cycle fatigue tests, the total dissipated energy density was evaluated as the sum of the areas formed within the hysteresis loops. This is a measure of the capacity of the material to absorb energy during seismic activity. After evaluating the total energy absorbed, the remaining energy

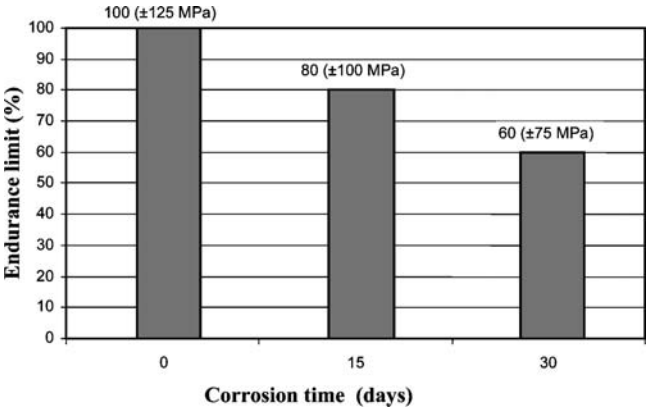

Fig. 7 Endurance limit variation versus time, for $BSt500_s$ steel

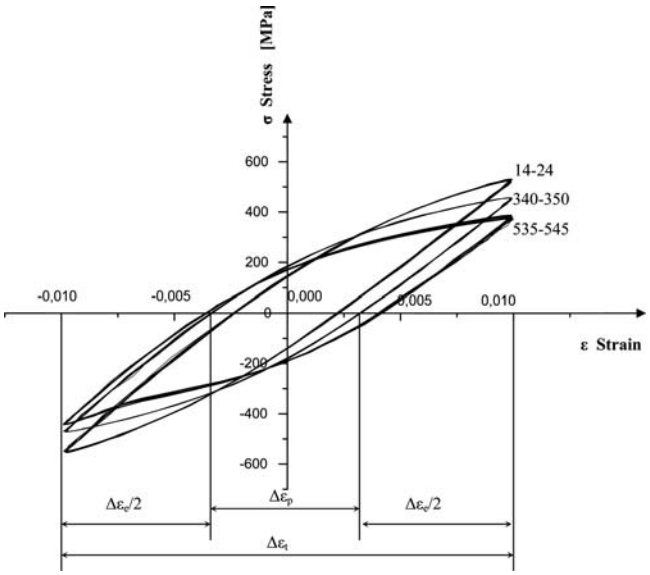

Fig. 8 Typical low cycle fatigue stress-strain diagrams, at ±1% applied strain, showing hysteresis loops for initial, middle, and final cycles for noncorroded steel

density was plotted after each cycle as a function of the number of subjected cycles.

Figure 9 shows that the inspection of steel reinforcement after 65% of the useful service life of noncorroded steel indicates that it is possible that a number of steel bars with an initial gage diameter of 12.15 mm, a corrosion level of >3.44%, and a remaining diameter of 11.94 mm will have already failed. For a more conservative inspection at 50% of the useful service life of the noncorroded steel, there is a possibility of partial reinforcement failure with the corrosion level exceeding 5.43% and a remaining diameter of 11.81 mm.

Figure 9 shows the correlation of the remaining energy density versus the imposed number of cycles after which the specified threshold is not met, as a proportion of the total number of cycles to failure of the noncorroded specimens.

Because the low-cycle fatigue tests were performed at constant strain amplitude, the maximum resisting force exerted by the specimens for each cycle is gradually reduced. Figures 8 and 10 show that a rapid drop of the applied force occurred during the first few cycles followed by a gradual reduction of this force for most of the life of the specimen, followed by a new rapid drop that continues until failure. Furthermore, an

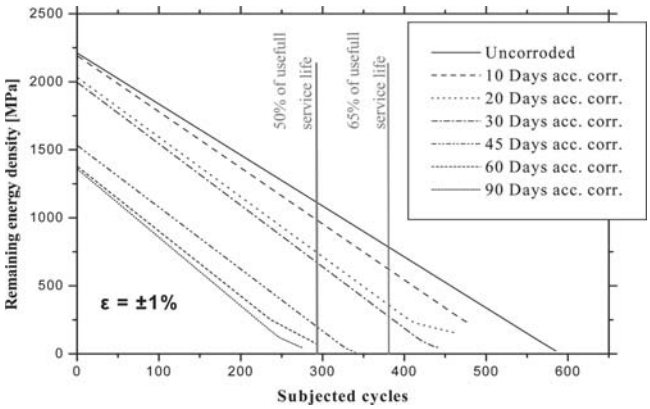

Fig. 9 Correlation of remaining energy density and subjected cycles for $\varepsilon = \pm 1\%$

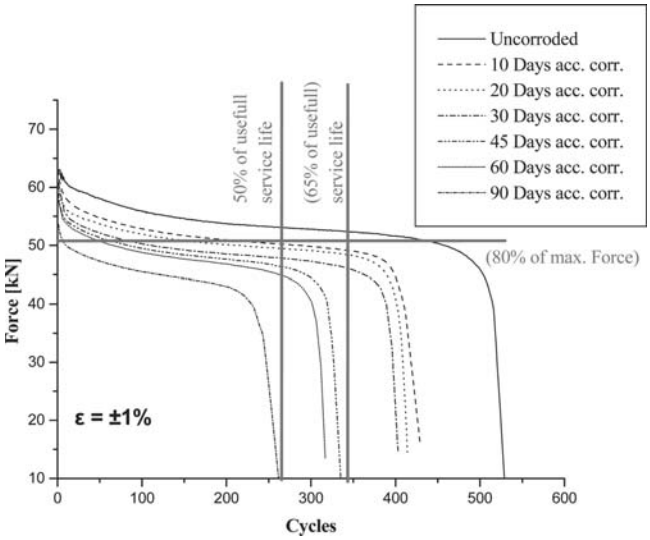

Fig. 10 Typical life expectancy of steel before the load capacity drops below 80% of the maximum value for ±1% of the strain level

overall reduction of the applied force is observed for the precorroded and postcorroded specimens, which was expected because the cross-sectional area was reduced with advancing corrosion. The reinforcing steel used in structures is expected to carry a constant load throughout its service life because these loads remain fairly constant over time. As may be seen from Fig. 10 and for a threshold of 80% of the maximum force of the noncorroded material and as the corrosion level increases, the remaining time for which the material can support this force is greatly reduced. Furthermore, if the number of cycles to failure is considered to be unaffected from corrosion, as is the case of code regulation that accounts for the use of steel reinforcement in concrete (Ref 28, 29), then failure may occur much sooner than expected.

Table 3 shows the failure behavior of the steel specimens versus the salt spray exposure duration, the total dissipated energy density, and the number of cycles to failure before and after the 80% threshold load limit.

3. Results

Corrosion was found to be an important factor for the integrity of steel, and pitting became evident after a few days of salt spray exposure and progressively more severe as the corrosion level increased. As the steel surface became rougher, cavities and notches were formed, which made the steel surface locally of smaller diameter than the average value. A considerable reduction in the fatigue limit took place because the mass loss led to a reduction of the exterior hard layer of martensite and a drastic drop in the energy density of the corroded specimens, thus developing stress concentration points that are highly localized at imperfections and especially in the pits and notches of the rib bases of the corroded steel. Thus, the increased corrosion led to a decrease of the useful life of the steel. From Fig. 2, it can be seen that the mass loss, constituting the wear rate, for corroded versus noncorroded 12 mm nominal steel specimens for levels of 15 and 30 days of corrosion were on the order of 1.5 to 2.9%, respectively. It was observed that a small mass loss created a great reduction in the strength and life expectancy of steel. In addition, a more detailed examination of the mass loss extended to a level of 90 days of corrosion was performed. The rib height was also measured during the different levels of corrosion, and after 90 days, corresponding to 8.26%, the average height of the ribs was reduced by approximately 80 to 85%.

Table 3 Low cycle fatigue failure behavior of precorroded and postcorroded steel with strain level ±1%

Duration of salt spray corrosion	Number of specimens	Total dissipated energy density, MPa	Cycles to failure	Cycles before load capacity drops below 80% of the maximum value
Uncorroded	3	2329	529	457
10 days	3	2262	429	280
20 days	3	2168	414	207
30 days	3	2117	403	108
45 days	3	1643	335	81
60 days	3	1430	317	64
90 days	3	1403	263	10

From Fig. 6, it can be seen that for steel corroded for 15 and 30 days, which corresponds to 1.5 and 2.9% mass loss, respectively, for a given applied stress (e.g., 125 MPa and stress ratio $R = -1$), their life expectancy is reduced to 3.5×10^6 and 1.95×10^6 cycles, respectively, from 8.1×10^6 cycles in the noncorroded case; in other words, the life expectancy of steel is reduced by approximately 56 to 76%. This is very significant for aggressive climatic conditions such as the ones existing in the coastal areas of Greece where salinity, high heat, humidity, and earthquakes are the predominant factors. Figure 11 shows the stress-strain curves versus the degree of corrosion and the energy density as the area under these curves. It can be seen that as the exposure time of the material to salt spray corrosion increases, not only the strength properties (i.e., the yield and fracture points) but also the ductility properties, such as energy density and elongation to fracture, decrease (Ref 11, 30). In harsh environments and seismic areas, steel bars of reinforced concrete structures must have great amounts of energy density, which is a property characterizing the damage tolerance potential of materials and may be used to evaluate the fracture under both static and dynamic fatigue-loading conditions (Ref 31). A considerable reduction in energy density is observed as the duration of corrosion is increased; the uncor-

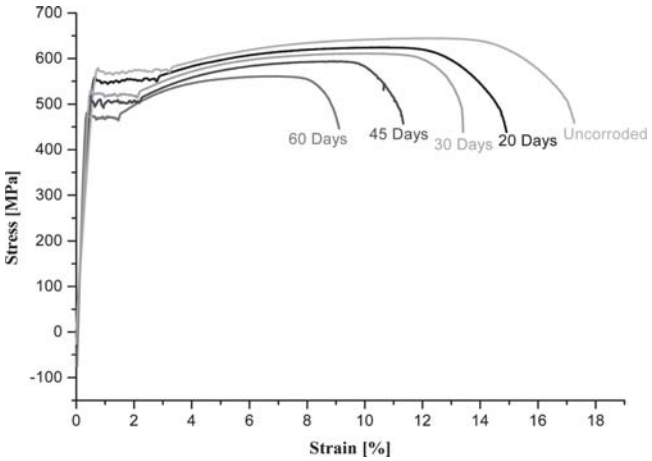

Fig. 11 Reduction of energy density for different corrosion levels

roded material has a greater energy deposit than any of the corroded bars, as shown by the area under the stress-strain curve. The energy deposit indicates the ability of a steel bar to absorb energy from external loads without danger of failure.

The endurance limit for corroded versus noncorroded steel specimens was reduced by 20 and 40%, respectively, for 15 and 30 days exposure time to salt spray according to Fig. 7, which is explained in a similar manner as that above.

The experimental results of uniaxial fatigue tests have shown an overall degradation of the corroded $BSt500_s$ steel reinforcing bars. The formation of an oxide layer on the surface of the specimens made them rougher by forming pits, notches, and cavities, thus allowing the formation of stress concentration points leading to cumulative damage under alternating fatigue loading. Furthermore, the oxide layer reduced the nominal cross-sectional area of the specimens. Considerable degradation of the steel specimens due to corrosion remains as a result of the drop in energy density (Fig. 9, 11) combined with the gradual loss of the exterior hard layer of martensite (Fig. 4).

4. Conclusions

A series of tests were performed to evaluate the effect of corrosion level on mass loss and on high and low cycle fatigue of $BSt500_s$ steel. The following conclusions were drawn:

- A direct correlation between corrosion and mass loss, for corroded versus noncorroded steel specimens for levels of corrosion for 15 and 30 days was found to be on the order of 1.5 to 2.9%, respectively. It was observed that a small mass loss created a great reduction in the strength and life expectancy of steel for low-cycle fatigue loading.
- From the experimental tests, it was observed that corrosion was initiated at the base of the ribs of the bars and that as the corrosion level increased the ribs were reduced. The rib height was reduced after each corrosion level and after 90 days, corresponding to an 8.26% mass loss, and the average height of the ribs was reduced by approximately 80 to 85%, which also has a direct impact on the bonding mechanism of reinforced concrete structures.
- Considerable reduction in the fatigue limit took place due to a reduction of the exterior hard layer of martensite and a drastic drop in the energy density of the corroded specimens, thus developing stress concentration points, which are highly localized at imperfections and especially in the pits and notches of the rib bases of the corroded steel. Thus, the increased corrosion led to a decrease in the useful life of the steel.
- The maximum load-bearing capacity was reduced during low-cycle fatigue loading, and further reduction was observed for corroded specimens. Older structures in earthquake-prone areas are not expected to display a constant load-bearing ability beyond a certain service life. The progression of corrosion caused a significant reduction of ductility and life expectancy.
- The endurance limit for corroded versus noncorroded steel specimens was reduced by 20 and 40%, respectively, for 15 and 30 days of exposure time to salt spray.
- Even though the impact of corrosion on the strength of steel is well known, the current design codes do not address the problem seriously because they are unable to quantify it and need further review. Further studies are needed to accumulate enough knowledge to justify a revision of these codes.

References

1. C. Fang, K. Lundgren, L. Chen, and C. Zhu, Corrosion Influence on Bond in Reinforced Concrete, *Cem. Concr. Res.,* 2004, **34,** p 2159-2167
2. G.J. Al-Sulaimani, M. Kaleemullah, I.A. Basunbul, and Rasheeduzzafar, Influence of Corrosion and Cracking on Bond Behaviour and Strength of Reinforced Concrete Members, *Proc. A.C.I.,* 1990, **2,** p 220-231
3. X. Fu and D.D.L. Chung, Effect of Corrosion on the Bond Between Concrete and Steel Rebar, *Cem. Concr. Res.,* 1997, **27**(12), p 1811-1815
4. R. Capozucca, Damage to Reinforced Concrete Due to Reinforcement Corrosion, *Constr. Build. Mat. J.,* 1995, **9**(5), p 295-303
5. Z.P. Bazant, Physical Model for Steel Corrosion in Concrete Sea Structures: Theory, *J. of the Engrg. Meth. Div., Proc. ASCE,* 1979, p 1137-1153
6. A.A. Almusallam, A.S. Al-Gahtani, A.R. Aziz, and Rasheeduzzafar, Effect of Reinforcement Corrosion on Bond Strength, *Constr. Build. Mat. J.,* 1996, **10**(2), p 123-129
7. A.A. Almusallam, A.S. Al-Gahtani, A.R. Aziz, F.H. Dakhil, and Rasheeduzzafar, Effects of Reinforcement Corrosion on Flexural Behavior of Concrete Slabs, *J. Mat. Civil Eng.,* 1996, **8**(3), p 123-127
8. G.M. Sheng and S.H. Gong, Investigation of Low Cycle Fatigue Behaviour of Building Structural Steels Under Earthquake Loading, *Acta Metall. Sinica,* 1997, **10**(1), p 51-55 (in English)
9. Y.H. Chai, Incorporating Low-Cycle Fatigue Model into Duration-Dependent Inelastic Design Spectra, *Earthquake Engng. Struct. Dyn.,* 2005, **34,** p 83-96
10. H. Shigeru, "Retrofitting of Reinforced Concrete Moment Resisting Frames," research report Dept. Civil. Engineering, Univ. of Canterbury, N.Z. (supervised by R. Park and H. Tanaka) ISSN0110-3326, 1995
11. C. Alk, M.P. Apostolopoulos, S.P. Papadopoulos, and G. Pantelakis, Tensile behavior of corroded reinforcing steel bars BSt 500s, *Constr. Build. Mat. J.,* 2006, **20**(9), p 782-789
12. C.J. Giovanni, A. Plizzari, Y. Du, D.W. Law, and C. Franzoni, Mechanical Properties of Corrosion-Damaged Reinforcement, *ACI Mater. J.,* 2005, **102**(2), p 256-264
13. G.C. Koch, M.P. Brongers, M.P. Thompson, Y.P. Virmani, and J.H. Payer, "Corrosion Costs and Preventive Strategies in the United States," Report No. FHWA-RD, Federal Highway Administration, Washington, DC, 2002
14. G.G. Clementa, "Testing of Selected Metallic Reinforcing Bars for Extending the Service Life of Future Concrete Bridges," Final Report VTRC 03-R7, Virginia Transportation Research Council, Charlottesville, VA, 2002
15. X. Wang and X. Liu, Bond Strength Modelling for Corroded Reinforcements, *Constr. Build. Mat. J.,* 2006, **20**(3), p 177-186

16. J.G. Cabrera, Deterioration of Concrete Due to Reinforcement Steel Corrosion, *Cem. Concr. Comp.,* 1996, **18**(l), p 47-59
17. P. Riva, A. Franchi, and D. Tabeni, Weld Tempcore Reinforcement Behavior for Seismic Applications, Materials and Structures, *Mater. Struct.,* 2001, **34,** p 240-247
18. A. Franchi, P. Riva, P. Ronca, R. Roberti, and M. La Vecchia, Failure Modalities of Reinforcement Bars in Reinforced Concrete Elements Under Cyclic Loadind, *Studi Ricerche.,* 1996, **17**, p 157-187
19. M. Pipa and A. Vercesi, "Cyclic Tests of Grade B400 and B500 Tempcore Bars" PREC8 Report, Laboratorio Nacional de Engenharia Civil, Technical University of Lisbon, 1996
20. M. Pipa, E.C. Carvalho, and A. Otes, "Experimental Behaviour of R.C. Beams with Grade 500 Steel," presented at 10th European Conference on Earthquake Engineering (Vienna, Austria), A.A. Balkema, 1994, p 2887-2892
21. P. Schiessl, "Corrosion of Steel in Concrete," Report TC 60-CSC, Réunion International des Laboratoires et Experts des Matériaux (RILEM), 1988
22. K. Stanish, R.D. Hooton, and S.J. Pantazopoulou, Corrosion Effects on Bond Strength in Reinforced Concrete, *ACI Struct. J.,* 1999, **96**(6), p 915-921
23. H.S. Lee, T. Noguchi, and F. Tomosawa, Evaluation of the Bond Properties Between Concrete and Reinforcement as a Function of the Degree of Reinforcement Corrosion, *Cem. Concr. Res.,* 2002, **32**(8), p 1313-1318
24. J.G. Cabrera and P. Ghoddoussi, Effect of Reinforcement Corrosion on the Strength of the Steel Concrete Bond, *International Conference, Bond in Concrete: from Research to Practice,* (Riga, Latvia), Faculty of Environmental Design, University of Calgary, Alberta, Canada, Vol 3, 1992, p 10.11-10.24
25. "Standard Practice for Operating Salt(Fog) Testing Apparatus," B 117-94, Section 3, Metal Test Methods, ASTM, 1995, p 1-8
26. "Standard Practice for Strain Controlled Fatigue Testing," E 606, *Annual Book of ASTM Standards,* ASTM, 1997, p 523-537
27. H.O. Fuchs and R.I. Stephens, *Metal Fatigue in Engineering,* John Wiley & Sons Inc, 1980, p 76-82
28. "Hellenic Anti-Seismic Code 2000 (EAK2000)," No. Δ17a/20.12.2000, Government Gazette ISSUE 2184B, Athens, Greece, 2001
29. CEN Technical Committee 250/SC8, EUROCODE 8: Earthquake Resistant Design of Structures: Part 1. General Rules and Rules for Buildings (ENV 1998-1-1/2/3), CEN, Berlin, Germany, 1995
30. Y.G. Du, L.A. Clark, and A.H.C. Chan, Effect of Corrosion on Ductility of Reinforcing Bars, *Mag. Concr. Res.,* 2005, 57(7), p 407-419
31. G.C. Sih and C.K. Chao, Failure Initiation in Unnotched Specimens Subjected to Monotonic and Loading, *Theor. Appl. Fract. Mech.*, 1984, **2,** p 67-73